

Cation- π Interactions as Determinants for Binding of the Compatible Solutes Glycine Betaine and Proline Betaine by the Periplasmic Ligand-binding Protein ProX from *Escherichia coli**

Received for publication, September 3, 2003, and in revised form, November 5, 2003
Published, JBC Papers in Press, November 11, 2003, DOI 10.1074/jbc.M309771200

André Schiefner^{‡§}, Jason Breed^{‡§¶}, Linda Bösser[¶], Susanne Kneip[¶], Jutta Gade[¶],
Gudrun Holtmann[¶], Kay Diederichs[‡], Wolfram Welte^{‡**}, and Erhard Bremer[¶]

From the [‡]Fachbereich Biologie, Universität Konstanz, Universitätsstrasse 10, D-78457 Konstanz, Germany and the [¶]Fachbereich Biologie, Laboratorium für Mikrobiologie, Philipps-Universität Marburg, Karl-von-Frisch Strasse, D-35032 Marburg, Germany

Compatible solutes such as glycine betaine and proline betaine are accumulated to exceedingly high intracellular levels by many organisms in response to high osmolarity to offset the loss of cell water. They are excluded from the immediate hydration shell of proteins and thereby stabilize their native structure. Despite their exclusion from protein surfaces, the periplasmic ligand-binding protein ProX from the *Escherichia coli* ATP-binding cassette transport system ProU binds the compatible solutes glycine betaine and proline betaine with high affinity and specificity. To understand the mechanism of compatible solute binding, we determined the high resolution structure of ProX in complex with its ligands glycine betaine and proline betaine. This crystallographic study revealed that cation- π interactions between the positive charge of the quaternary amine of the ligands and three tryptophan residues forming a rectangular aromatic box are the key determinants of the high affinity binding of compatible solutes by ProX. The structural analysis was combined with site-directed mutagenesis of the ligand binding pocket to estimate the contributions of the tryptophan residues involved in binding.

The water content of bacterial cells is determined solely by osmotic processes as bacteria lack systems for active water transport into or out of the cell in response to an increase or a decrease of osmolarity in the environment (1, 2). To cope with hyperosmotic conditions, non-halophilic microorganisms generally amass large quantities of a particular group of organic osmolytes, the so-called compatible solutes (3), either by *de novo* synthesis or by direct uptake from the environment (1, 4–7). Compatible solutes are operationally defined as organic

osmolytes that can be accumulated by the cell to exceedingly high concentrations without disturbing vital cellular functions or the correct folding of proteins (3). Their intracellular accumulation counteracts the osmotic efflux of water from the cell and thus contributes to the restoration of turgor (8) and the resumption of growth of the bacterial cells under conditions of low water activity. In addition to contributing to the maintenance of cellular water content at high external osmolarities (9), compatible solutes also counteract destabilization of native structures of proteins upon freezing, heating, desiccation, and exposure to high ionic strength both *in vitro* and *in vivo* (10–15).

The intracellular accumulation of compatible solutes as a strategy for adaptation to high osmolarity has been widely adopted not only by bacteria (5) and Archaea (16, 17) but also by fungal, plant, animal, and even human cells (18–20). Moreover a few classes of compounds are used universally throughout the kingdoms, reflecting fundamental constraints on the type of solutes that are compatible with macromolecular and cellular functions (16, 21, 22). One of the most ubiquitous compatible solutes used both by prokaryotic and eukaryotic cells, is the trimethylammonium compound glycine betaine (*N,N,N*-trimethylglycine, GB).¹ The exact biochemical mechanism(s) through which compatible solutes act as protein stabilizers is not completely understood. Their functioning is generally explained in terms of the preferential exclusion model (23). This hypothesis predicts that compatible solutes are excluded from the immediate hydration shell of proteins, which is apparently due to unfavorable interactions with protein surfaces (24, 25). This causes a non-homogeneous distribution of compatible solutes within the cell water and a preferential hydration of protein surfaces. Experimental verification came from neutron diffraction studies (26). The nonuniform distribution of compatible solutes within the cell water results in a thermodynamic force that drives proteins to occupy a smaller volume to reduce the amount of excluded water, thereby stabilizing the native structure of proteins.

Many Gram-negative and Gram-positive bacterial species that have been found to accumulate GB are able to acquire this compatible solute from environmental sources through high affinity transport systems (1, 6, 27, 28). GB transport in *Escherichia coli* is under osmotic control (27, 29, 30) and is mediated by two transport systems: the single component H⁺-compatible

* This study was supported by Deutsche Forschungsgemeinschaft Grant SFB-395, by the Graduiertenkolleg "Proteinfunktion auf atomarer Ebene," by the Max-Planck-Institute for terrestrial Microbiology (Marburg), and by the Fonds der Chemischen Industrie (to E. B.). The costs of publication of this article were defrayed in part by the payment of page charges. This article must therefore be hereby marked "advertisement" in accordance with 18 U.S.C. Section 1734 solely to indicate this fact.

The atomic coordinates and structure factors (codes 1R9L and 1R9Q) have been deposited in the Protein Data Bank, Research Collaboratory for Structural Bioinformatics, Rutgers University, New Brunswick, NJ (<http://www.rcsb.org/>).

§ Both authors contributed equally to this work.

¶ Present address: Astra Zeneca, Mereside, Macclesfield SK10 4TG, UK.

** To whom correspondence should be addressed. E-mail: wolfram.welte@uni-konstanz.de.

¹ The abbreviations used are: GB, glycine betaine (*N,N,N*-trimethylglycine); PB, proline betaine (*N,N*-dimethyl-L-proline); X-gal, 5-bromo-4-chloro-3-indolyl- β -D-galactopyranoside; PIPES, 1,4-piperazine diethanesulfonic acid; NCBI, National Center for Biotechnology Information.

solute cotransporter ProP (31) and the multicomponent transport system ProU (32, 33). The ProU system is a member of the ATP-binding cassette superfamily (34, 35) consisting of two cytoplasmic, membrane-associated ATPases, ProV; two integral membrane proteins, ProW; and a periplasmic ligand-binding protein, ProX (33). Access of GB present in the environment to the periplasmic ProX protein is provided by passive diffusion across the outer membrane through the OmpC and OmpF general porins of *E. coli* (36). ProX binds GB avidly with a K_D of $\sim 1 \mu\text{M}$ (32, 37, 38) delivering the ligand to the substrate translocation complex that is embedded in the cytoplasmic membrane. Driven by ATP hydrolysis, the translocation complex then transports the ligand into the cytoplasm (34, 35, 39). In addition to GB, the ProU transporter also serves as a high affinity uptake system for proline betaine (*N,N*-dimethyl-L-proline, PB), and this compatible solute is recognized by the ProX protein with high affinity ($K_D = 5 \mu\text{M}$) as well (38). ProU also functions as an uptake system for a variety of other compatible solutes (e.g. proline and ectoine), but in contrast to GB and PB none of these compounds appear to be recognized by the ProX protein (37, 38, 40).

The substrate-binding protein binds its ligand(s) selectively and with high affinity, which is thought to ensure the substrate specificity and directionality of the overall transport reaction for a given binding protein-dependent transport system (35). Periplasmic binding proteins are generally composed of two domains connected by one to three polypeptide chains forming a hinge between them. In the ligand-free open conformation the two rigid domains are flexibly linked by the hinge. This has been shown by the structural analysis of various open states of the ribose-binding protein and D-allose-binding protein (41, 42). Ligand binding induces a large conformational change in the hinge region that moves both domains toward each other. After this domain movement the ligand is engulfed in a predefined cleft between the two domains that refers to the closed conformation of the binding protein.

Compatible solutes are apparently preferentially excluded from the immediate hydration shell of proteins (23–25). Yet a ligand-binding protein such as ProX binds the compatible solutes GB and PB with high affinity and high specificity (32, 37, 38, 43). This observation raises the question as to how such a high affinity interaction between a compatible solute and a protein can take place. To understand the molecular determinants that govern substrate recognition and binding of compatible solutes by ProX, we determined the high resolution crystal structure of the ProX protein in complex with each of its ligands, i.e. ProX-GB and ProX-PB. This crystallographic analysis was combined with site-directed mutagenesis of the residues forming the ligand binding pocket of ProX to determine their relative importance for high affinity binding of the compatible solute GB by the ProX protein from *E. coli*. The analysis revealed cation- π interactions between the quaternary amine of GB and PB and the indole groups of three tryptophan residues.

EXPERIMENTAL PROCEDURES

Overproduction and Purification of Wild-type and Mutant ProX Protein—The wild-type *E. coli* ProX protein was overproduced and purified to homogeneity essentially as described previously (44). In brief, the *proX* gene was overexpressed under the control of the bacterial phage T7 ϕ 10 promoter present on the *proX*⁺ low copy number plasmid pSK7 (Cm^r) in the *E. coli* strain PD141 (λ DE3) (44). This strain harbors a chromosomal copy of the gene for the phage T7 RNA polymerase under the control of an isopropyl-1-thio- β -D-galactopyranoside-inducible *lacPOLLacI* promoter system, thereby allowing the selective expression of the *proX* gene present on plasmid pSK7 from the T7 ϕ 10 promoter upon the addition of isopropyl-1-thio- β -D-galactopyranoside to the cell culture. Cells of strain PD141 (λ DE3) (pSK7) were grown in a minimal medium (44) in the presence of 30 $\mu\text{g ml}^{-1}$ chloramphenicol because components of rich media (e.g. yeast extract) are known to contain GB

(45) that could potentially be scavenged and bound by ProX. In this way we ensured that the purified ProX protein was free of ligand since the *E. coli* strains used for overproduction are unable to synthesize GB. Overproduction of ProX was initiated by the addition of 1 mM isopropyl-1-thio- β -D-galactopyranoside when the cell culture had reached an A_{578} of ~ 1.0 – 1.5 . After 1 h of further growth, the cells were harvested by centrifugation, and the periplasmic proteins were released from the cells by cold osmotic shock (46). Insoluble material was removed from the released periplasmic proteins by ultracentrifugation, and the supernatant was then subjected to fast protein liquid chromatography on a DEAE-Sepharose fast flow column (Amersham Biosciences). Proteins were eluted from this anion exchange column with an increasing Tris-HCl (pH 8.3) gradient (16–400 mM). ProX-containing fractions were combined, and ammonium sulfate was added to a final concentration of 1.5 M. This protein solution was then subjected to hydrophobic interaction chromatography on a phenyl-Sepharose column (Amersham Biosciences). The ProX protein was eluted with a decreasing ammonium sulfate gradient (1.5–0 M ammonium sulfate dissolved in 10 mM Tris-HCl, pH 8.3). The purified ProX protein was then dialyzed overnight against 5 liters of 10 mM Tris-HCl (pH 7.3) buffer. The ProX protein was free from other contaminating proteins as judged from SDS-polyacrylamide gels stained with Coomassie Brilliant Blue.

ProX proteins with mutations in the substrate binding site were purified essentially as wild-type ProX protein except that the *E. coli* strain LinE2 (PD141 Δ (*proU::spc*)608) was used for the overexpression of the mutant *proX* genes present on derivatives of plasmid pSK7. Strain LinE2 carries a chromosomal deletion of the entire *proU* operon (38), thereby avoiding the contamination of the mutant ProX protein preparations with the wild-type ProX protein during protein purification.

Genetic Construction of Bacterial Strains for Expression of Mutant ProX—To construct an *E. coli* strain that lacked the *E. coli proU* operon and that would allow phage T7 ϕ 10-mediated overexpression of plasmid-encoded mutant *proX* genes, we prepared a P1vir lysate (47) on the *proU-lacZ* fusion strain BK16 (MC4100 ϕ (*proU-lacZ*)hyb2 λ placMu15 (Kan^r)).² Using this phage lysate, we transduced the *lacZ* gene fusion positioned next to the λ placMu15 (Kan^r) prophage (49) into the *E. coli* strain PD141 (MC4100 (λ DE3))³ by selecting for kanamycin-resistant colonies (50 $\mu\text{g ml}^{-1}$) in the presence of X-gal (300 $\mu\text{g ml}^{-1}$) on Luria Bertani (LB) agar plates. One of these transductants was strain LinE1. We then replaced the ϕ (*proU-lacZ*)hyb2 λ placMu15 (Kan^r) prophage in strain LinE1 with the Δ (*proU::spc*)608 deletion from strain MKH13 (38) by transducing strain LinE1 with a P1vir lysate prepared on strain MKH13 and selecting for spectinomycin-resistant colonies (100 $\mu\text{g ml}^{-1}$) in the presence of X-gal on LB agar plates. The desired transductants carrying the Δ (*proU::spc*)608 deletion were identified as spectinomycin-resistant colonies that were kanamycin-sensitive and LacZ⁻. One of these transductants was strain LinE2. The absence of the ProX protein from strain LinE2 was verified by Western blotting analysis using a ProX antiserum and whole cell extracts prepared from cells grown in the presence of 250 mM NaCl in minimal medium.

Site-directed Mutagenesis of the *proX* Gene—To probe the contributions of residues Trp⁶⁵, Trp¹⁴⁰, and Trp¹⁸⁸ in ProX to GB binding, we mutated the corresponding codons in the *proX* gene via site-directed mutagenesis using the QuikChange® site-directed mutagenesis kit (Stratagene) and custom synthesized primers (MWG-Biotech) containing the desired mutations. We replaced the codon for each of these Trp residues in *proX* with codons encoding the amino acids Ala, Leu, Phe, Tyr, Asp, or Glu in plasmid pSK7 by following the protocol provided by Stratagene. The entire coding region of the mutant *proX* genes was then sequenced to ensure the presence of the desired mutation and the absence of unwanted alterations in the *proX* coding region. DNA sequencing was carried out by the chain terminating method (51) with the Thermo Sequenase fluorescent labeled primer cycle sequencing kit (Amersham Biosciences). The DNA sequencing reactions were primed with synthetic oligonucleotides labeled at their 5' end with the infrared dye IRD-800 (MWG-Biotech), and the products were analyzed using a LI-COR DNA sequencer (model 4000, MWG Biotech). Each of the mutant *proX* alleles chosen for overproduction of the altered ProX proteins contained only the desired mutations in the codons encoding residues Trp⁶⁵, Trp¹⁴⁰, or Trp¹⁸⁸ (pLB2, W188A; pLB3, W188L; pLB4, W188F; pLB5, W188Y; pLB6, W140A; pLB7, W140L; pLB8, W140F; pLB9, W140Y; pLB10, W65A; pLB11, W65L; pLB12, W65F; pLB13, W65Y; pLB14, W188D; pLB15, W188E; pLB16, W140D; pLB17, W140E; pLB18, W65D; and pLB19, W65E). A double mutant containing replace-

² B. Kempf and E. Bremer, unpublished results.

³ P. Dersch and E. Bremer, unpublished results.

TABLE I
Intensity statistics of the heavy atom derivatives and native data sets

	Data set			
	Derivative		Native	
	(CH ₃) ₃ PbAc	CH ₃ HgCl	Glycine betaine	Proline betaine
Ligand	Glycine betaine	Glycine betaine	Glycine betaine	Proline betaine
Wavelength (Å)	1.54179	1.54179	0.8439	1.54179
Total rotation range (°)	100	100	90	100
Temperature (K)	291	291	100	291
Cell (<i>a</i> , <i>b</i> , <i>c</i>) (Å)	48.0, 55.0, 115.8	47.9, 55.1, 115.7	47.59, 53.86, 115.43	47.71, 54.98, 115.73
Resolution limits (Å)	20.0–2.48 (2.55–2.48)	20.0–2.48 (2.60–2.48)	15–1.57 (1.67–1.57)	15–2.05 (2.25–2.05)
Number of reflections	43,801	43,602	142,884	75,377
Unique reflections	20,031	20,826	40,866	19,587
Completeness (%)	95.4 (95.1)	99.2 (99.5)	96.6 (95.2)	99.0 (99.4)
<i>I</i> / σ <i>I</i>	15.7 (6.3)	19.0 (10.0)	30.0 (18.6)	15.1 (5.65)
<i>R</i> _{sym}	4.1 (12.0)	2.8 (6.7)	2.6 (4.7)	6.0 (23.9)
<i>R</i> _{meas} ^a	5.3 (15.5)	3.6 (8.8)	3.0 (5.5)	6.6 (27.5)
<i>R</i> _{mrgd-F} ^a	6.4 (16.6)	3.6 (7.9)	2.2 (4.8)	7.7 (23.3)
B-factor Wilson plot (Å ²)	27.8	32.4	7.7	33.3
Phasing power overall	1.39	1.33		
Figure of merit overall	0.62			

^a *R*_{meas} and *R*_{mrgd-F} are better indicators for data quality than *R*_{sym}. *R*_{meas} is redundancy-independent, and *R*_{mrgd-F} is a measure for the quality of the reduced amplitudes (48, 50).

ments of the amino acids at positions Trp⁶⁵ and Trp¹⁴⁰ were constructed by remutating plasmid pLB10 to yield plasmid pLB20 (W65A,W140A). The mutant *proX* pLB plasmids were each introduced by electroporation into the *E. coli* strain LinE2 (Δ (*proU::spc*)608), and 4 liters of minimal medium with 0.4% (w/v) glucose as the carbon source were used for the overproduction of the mutant ProX proteins. Usually we obtained between 10 and 20 mg of purified ProX protein from 4 liters of cell culture.

Binding of Radiolabeled GB to ProX and Its Mutant Derivatives—The binding affinity of the wild-type ProX protein and its mutant derivatives constructed by site-directed mutagenesis of *proX* was measured by using an ammonium sulfate precipitation assay (52). Purified ProX protein (5 μ M, determined using the BCA assay) was incubated with nine different concentrations of radiolabeled GB (1, 2, 5, 7, 10, 20, 30, 50, and 110 μ M) in a 100- μ l reaction volume of 10 mM Tris-HCl (pH 7.3) for 5 min at room temperature. Then the ProX protein was precipitated with 900 μ l of ice-cold saturated ammonium sulfate solution. After an incubation of 10 min on ice, the precipitated ProX protein was collected by filtration onto a nitrocellulose filter (pore size, 0.45 μ m; Schleicher & Schuell), the filter was then washed with 10 ml of an ice-cold ammonium sulfate solution, and the radioactivity retained by ProX on the filter was determined by scintillation counting. Each measurement was repeated three times for each concentration to determine the binding constant and the S.D. A mutant is treated as non-binding if no binding, either specific or unspecific, occurs at a concentration of 110 μ M GB (Table III). According to the properties of the compatible solute GB presented in the Introduction, we do not expect unspecific binding of GB to ProX at this rather low concentration.

Data Collection and Structure Refinement—Crystals of ProX-GB and ProX-PB were grown by vapor-phase equilibration at 18 °C as described previously (44). In brief, protein (10 mg/ml in 10 mM Tris, pH 8.3) was diluted 1:1 with a reservoir solution containing 26–28% (w/v) polyethylene glycol 4000 and 50 mM PIPES, pH 6.2–6.4. The crystals grew within 4–6 weeks and belong to the space group P2₁2₁2₁ with unit cell parameters of *a* = 48.0, *b* = 55.0, and *c* = 115.7 Å containing one monomer per asymmetric unit. In complex with GB, ProX crystals were quite resistant to damage by heavy atoms; both high concentrations and long soak times were possible. Two derivative crystals of ProX-GB were obtained by soaking of the crystals either with 10 mM methylmercuric(II) chloride (CH₃HgCl) for 48 h or with 5 mM trimethyllead acetate ((CH₃)₃PbAc) for 72 h at room temperature. Data sets of the derivative crystals and a native crystal of ProX-PB were collected at room temperature using a rotating anode generator (Schneider, Offenburg, Germany) equipped with a Mar345 imaging plate detector (MarResearch, Hamburg, Germany). A native data set of ProX-GB was collected at the European Molecular Biology Laboratory outstation Deutsches Elektronen Synchrotron Hamburg beamline BW7B under cryogenic conditions. For this purpose the crystals were soaked in reservoir solution with stepwise increasing glycerol concentrations up to a final concentration of 25% (v/v) glycerol and then transferred to liquid nitrogen. All data sets were processed using XDS (53) as summarized in Table I. Heavy atom positions and initial phases were calculated using SOLVE

(54) followed by solvent flattening using DM (55). Chain tracing and model building was done with the graphical interface O (56) followed by alternating cycles of model building and refinement using REFMAC5 (57). The quality of the obtained models was validated with the program PROCHECK (58). Figures with molecule presentations were prepared with the programs MolScript (59), BobScript (60), and Raster3D (61).

Sequence Analysis—DNA and protein sequences were assembled and analyzed with the Lasergene program (DNASTAR, Ltd.) on an Apple Macintosh computer. Searches for protein homologues to the *E. coli* ProX protein were performed at the National Center for Biotechnology Information (NCBI) by using the BLAST programs with standard values (62). Protein sequences were aligned with the Clustal algorithm provided with the Lasergene program.

Chemicals—GB and PB were purchased from Sigma and Extrasynthèse, respectively. Radiolabeled GB ([1-¹⁴C]glycine betaine, 55 Ci mmol⁻¹) was obtained from American Radiolabeled Chemicals Inc. (St. Louis, MO).

RESULTS

Overall Structure—The structure of ProX from *E. coli* has been solved in the closed conformation in complex with each of the two ligands, GB and PB. Initial phases for ProX-GB were obtained by multiple isomorphous replacement using two heavy atom derivatives, CH₃HgCl and (CH₃)₃PbAc (see Table I). After solvent flattening the maps were sufficiently clear to trace the polypeptide. The initial model was refined against a native ProX-GB data set to 1.6-Å resolution. Clear difference electron density could be seen for the bound ligand. The final model contains all 309 residues of the mature protein, a bound GB, and a metal ion (see Table II). The corresponding structure of ProX-PB was solved by molecular replacement with the former structure (see Table II).

ProX-GB and ProX-PB are ellipsoidal with approximate dimensions of 75 × 38 × 20 Å³. The structure can be subdivided into two globular domains: domain A (*blue*) from residues 1–92 and 234–309 and domain B (*yellow*) from residues 93–233 connected by the two switch segments, residues 90–94 and 231–235, forming the hinge region (Fig. 1). Each domain consists of a four-stranded β -sheet flanked by α -helices on both sides as usually found among the members of the binding protein family.

In general binding proteins are subdivided into two structural groups with the different domain folds I and II, which correlate with the number of switches of the polypeptide between the two domains (63). Group one shows three switches, and group II shows two switches. An additional group is represented by the structures of FhuD and BtuF from *E. coli*,

TABLE II
Refinement statistics of the native structures

	Glycine betaine	Proline betaine
Resolution limits (Å)	12.26–1.59	15.0–2.05
Total number of reflections	39,378	19,430
Reflections in working set	37,409	18,626
Reflections in test set	1,969	804
R (%)	15.0	17.2
R_{free} (%)	18.6	21.3
No. of amino acid residues	309	309
No. of protein atoms	2,390 ^a	2,382
No. of metal ions	1	1
No. of water molecules	429	59
No. of ligand atoms	8	10
B-factor for all atoms (Å ²)	13.5	29.0
B-factor of protein atoms (Å ²)	11.7	29.0
r.m.s.d. ^b bonds (Å)	0.013	0.010
r.m.s.d. angles (°)	1.385	1.239

^a Side chains of Asn⁹⁰ and Met¹⁶⁹ are modeled in two alternate conformations.

^b r.m.s.d., root mean square deviation.

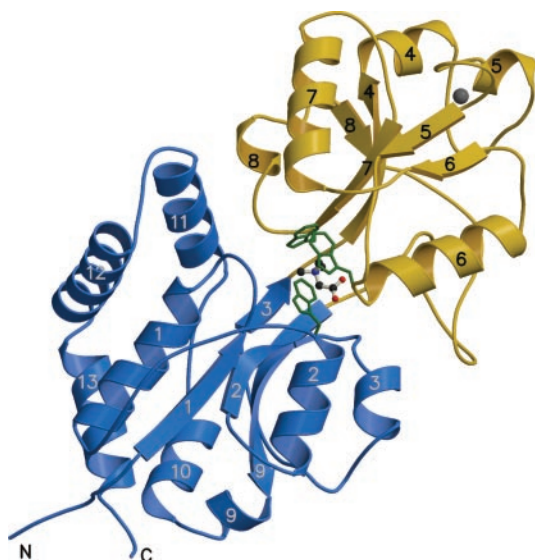


FIG. 1. **Ribbon diagram of ProX.** Domain A (residues 1–92 and 234–309) and domain B (residues 93–233) are colored *blue* and *yellow*, respectively. The two switch segments, residues 90–94 and 231–235, connect both domains. Helices and strands are consecutively numbered, and the N and C termini are labeled at the *bottom*. The ligand GB is drawn as a *ball-and-stick* and is enclosed by the three Trp residues (*green*) involved in ligand binding.

periplasmic binding proteins specific for ferrichrome and vitamin B₁₂, respectively (64, 65). These proteins have only one switch between their two domains. According to this classification ProX has a periplasmic binding protein type II fold.

The Ligand Binding Site—As expected from other binding protein structures, the ligand binding site is located in the cleft between the two globular domains (Fig. 1). The two adjacent switch segments in the hinge region allow the formation of a deep cleft that entirely buries the betaine ligand and thus prevents it from contacting the solvent.

Around the quaternary amine of the betaine ligand, the binding pocket is formed by the indole groups of the three tryptophans Trp⁶⁵, Trp¹⁴⁰, and Trp¹⁸⁸. Fig. 2 shows the electron density for the GB ligand surrounded by the tryptophan residues refined at 1.6-Å resolution. These planar indole groups are arranged like three faces of a rectangular box with the planes of Trp⁶⁵ and Trp¹⁴⁰ being almost parallel to each other, while that of Trp¹⁸⁸ is perpendicular to these.

Trp⁶⁵ at the C terminus of strand 2 is the only one of the tryptophans provided by domain A and is closest to the switch

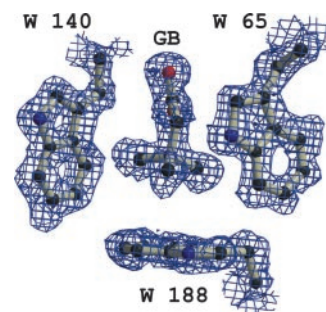


FIG. 2. **Electron density of the tryptophan box.** Shown is the binding pocket of ProX-GB with $2F_o - F_c$ map contoured at 1σ after refinement to 1.6-Å resolution. The tryptophan residues form a rectangular box with Trp¹⁸⁸ as the bottom and Trp⁶⁵ and Trp¹⁴⁰ as the sides.

segments (Fig. 3). Domain B provides the other two tryptophan residues Trp¹⁴⁰ and Trp¹⁸⁸. Trp¹⁸⁸ is placed at the C-terminal end of strand 7, and Trp¹⁴⁰ is furthest from the switch segments and located in the loop between strand 5 and helix 6, which apparently is stabilized by the disulfide bond between Cys¹³⁶ and Cys¹⁴².

This disulfide bond between Cys¹³⁶ and Cys¹⁴² is close to the ligand binding site. Whereas other binding protein structures such as putrescine-binding protein, dipeptide-binding protein, leucine-binding protein, and leucine/isoleucine/valine-binding protein with Protein Data Bank accession codes 1A99, 1DPE, 2LPB, and 2LIV, respectively (66), also contain disulfide bonds, all of these are placed distantly from the ligand binding site.

The carboxylic group of the GB ligand protrudes out of the indole box forming hydrogen bonds with the backbone amide hydrogens of Gly¹⁴¹ and Cys¹⁴² of domain B. These two residues are part of the loop between the disulfide-linked residues Cys¹³⁶ and Cys¹⁴², which also contains the indole ring of Trp¹⁴⁰. Additionally the carboxylic group forms a hydrogen bond with the imidazole ring of His⁶⁹ from domain A (Fig. 3).

Residues involved in the binding of PB are essentially the same as can be seen in Fig. 4 showing a superposition of the ProX-PB structure (ligand, *yellow*) onto the ProX-GB structure (ligand, *blue*). The two methyl groups, C-1 and C-2, as well as the C δ (from the proline ring) of the quaternary amine form similar contacts with the three indole rings, and the carboxylic group forms hydrogen bonds identical to those in ProX-GB. Also the PB ring atoms C β and C γ contribute additional van der Waals interactions with the indole ring of Trp⁶⁵ and C γ with Leu⁶⁸ side chain as well.

Mainly there are two contributions involved in the binding of a quaternary ammonium group in an aromatic environment, cation- π and van der Waals interactions. To understand the nature of the interaction between the tryptophans and the ligand, all distances between the carbon atoms bonded to the quaternary nitrogen and the ring atoms of the three indole groups were determined (Fig. 5). These distances were compared with a compiled list of van der Waals radii published by Li and Nussinov (67). If the influence of the quaternary ammonium charge on the contact distances is neglected, the methyl or methylene groups and the aromatic ring atoms possess van der Waals radii of 1.92 and 1.82 Å, respectively. This results in a mean distance of 3.74 Å between those carbon atoms having a S.D. of ~ 0.5 Å (67). We therefore consider an indole ring atom to be in contact with a methyl or a methylene group if their mutual distance is between 3.5 and 4 Å. The indole ring atoms that fulfill this criterion are color-coded in Fig. 5. According to this criterion, GB forms nine, five, and four contacts with Trp¹⁸⁸, Trp⁶⁵, and Trp¹⁴⁰ indole groups, respectively. The number of contacts of the indole rings suggests that the three indole groups contribute differently to the enthalpy of GB binding.

FIG. 3. **Stereopicture of the binding pocket.** Domains are colored *blue* and *yellow* as in Fig. 1. The ligand GB and residues involved in binding are drawn as *ball-and-stick* and labeled with residue name and number. Hydrogen bonds are represented as *dashed lines*, whereas the cation- π interaction is not explicitly depicted. The side chain of Cys¹⁴² is not drawn to improve clarity.

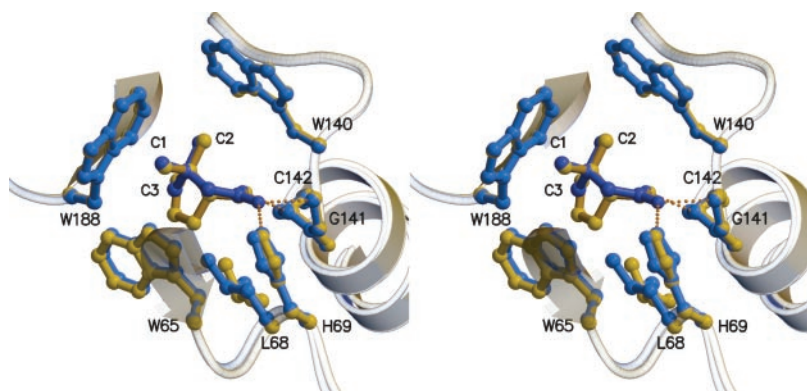
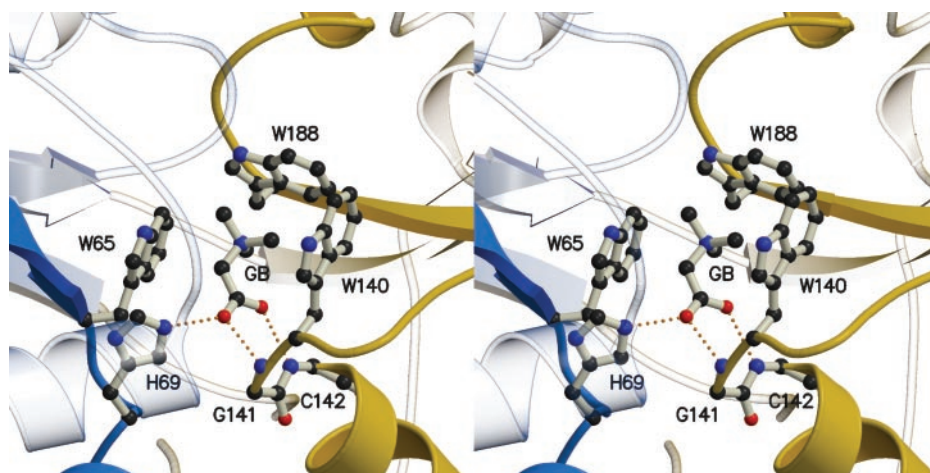


FIG. 4. **Stereopicture of the superposition of ProX-PB (yellow) onto ProX-GB (blue).** The C α positions of the Trp⁶⁵, Trp¹⁴⁰, and Trp¹⁸⁸ were used to superimpose the ligand binding sites. Secondary structure elements are shown for side chains involved in ligand binding; moreover the point of view has been changed to improve clarity. Additionally Leu⁶⁸, which is suitably spaced to form van der Waals contacts with the C γ atom of the ring structure of proline, is shown. The methyl groups of the ligand are labeled according to the numbers of the ProX-GB structure in the Protein Data Bank file (C-3 = C δ in ProX-PB).

Trp¹⁸⁸ is contacted by each of the three methyl groups because the C α -N bond is oriented perpendicular to the aromatic bottom of the box (Fig. 3). Trp⁶⁵ is contacted by the methyl group C-1 and the C α , and Trp¹⁴⁰ is contacted only by the methyl group C-2.

In the case of PB, seven, two, and five contacts are found of the quaternary amine with the indole rings of Trp¹⁸⁸, Trp⁶⁵, and Trp¹⁴⁰, respectively. One difference compared with the ProX-GB structure is that the C α is no longer in contact distance with the indole ring of Trp⁶⁵, having been pushed aside by the PB ring atoms C β and C γ . These ring atoms form nine new van der Waals contacts with Trp⁶⁵, colored *green* in Fig. 5 because they are not part of the quaternary amine.

Metal Binding Site—A metal binding site distant from the ligand binding site has been identified in the ProX structure. The metal ion is shown in Fig. 1 as a *gray sphere* in domain B between helix 5 and strand 5. Although the protein was never exposed to a buffer containing any metal cations during purification and crystallization an ion has been identified in the loop from residues 125 to 130. An anomalous difference electron density shows a strong peak of 14.5 σ at $\lambda = 0.8439$ Å. The octahedral coordination of the ion is provided by five ligands of the surface-exposed loop in domain B between helix 5 and strand 5 (Asp¹²⁴, Asn¹²⁶, Asp¹²⁸, Lys¹³⁰-CO, and Asp¹³²) and completed by a water molecule as the sixth ligand. This arrangement of the binding site resembles an EF-hand motif. A similar situation has been found in the alginate-binding protein where the metal ion has been identified to be calcium (68). Whereas the coordination of the metal is rather indicative for a calcium ion the anomalous signal at the measured wavelength is pointing to a transition metal. It was not possible to decide which metal is actually bound by ProX. The loop from residues 125 to 130 that is apparently stabilized by the metal ion seems to have no function.

Differentiation of the Three Indole Groups as Assessed by Mutations and Structural Data—To estimate the contributions of each of the indole groups of the tryptophan box, site-specific mutants were designed, and their relative binding affinity for GB was compared with that of the wild type. The binding affinity for the wild-type ProX measured by the ammonium sulfate precipitation is in very good agreement with a K_D value of 1.4 μ M determined by a release assay (32). All three tryptophan residues were consecutively substituted by tyrosine, phenylalanine, alanine, leucine, aspartate, or glutamate as summarized in Table III. The data demonstrate that a phenyl ring can provide a contribution to the binding affinity similar to that of an indole ring ($K_D = 3$ –5 μ M). In contrast, non-aromatic replacements of these residues impair the binding affinity considerably. The strongest influence of non-aromatic mutations is at position 188 where no binding affinity is detectable in the Ala, Leu, Asp, and Glu mutants. Position 65 is to a certain degree tolerant against Ala ($K_D = 50$ μ M) but does not tolerate leucine and acidic residues, whereas position 140 tolerates Ala, Leu, Asp, and Glu substitutions with dissociation constants being 2–10 times larger than for the wild type (Table III). Thus, the binding affinity is most sensitive against substitutions at position 188. The weakest sensitivity is at position 140 confirming the relative importance of the single tryptophans derived from the number of contacts with the GB (Fig. 5). Nevertheless the two residues Trp⁶⁵ and Trp¹⁴⁰ are necessary for the binding as seen from the double mutant W65A,W140A (see Table III).

A Conserved Sequence Motif—A BLAST search in the NCBI data base identified many proteins that are homologous to ProX. For clarity we selected a few representatives of the taxonomic classes. The selection is shown in Fig. 6; the *E. coli* sequence is followed by sequences of three Enterobacteriaceae (same family), one Vibrionales (same subdivision), three Pseudomonales (same subdivision), one Rhodospirillales (same

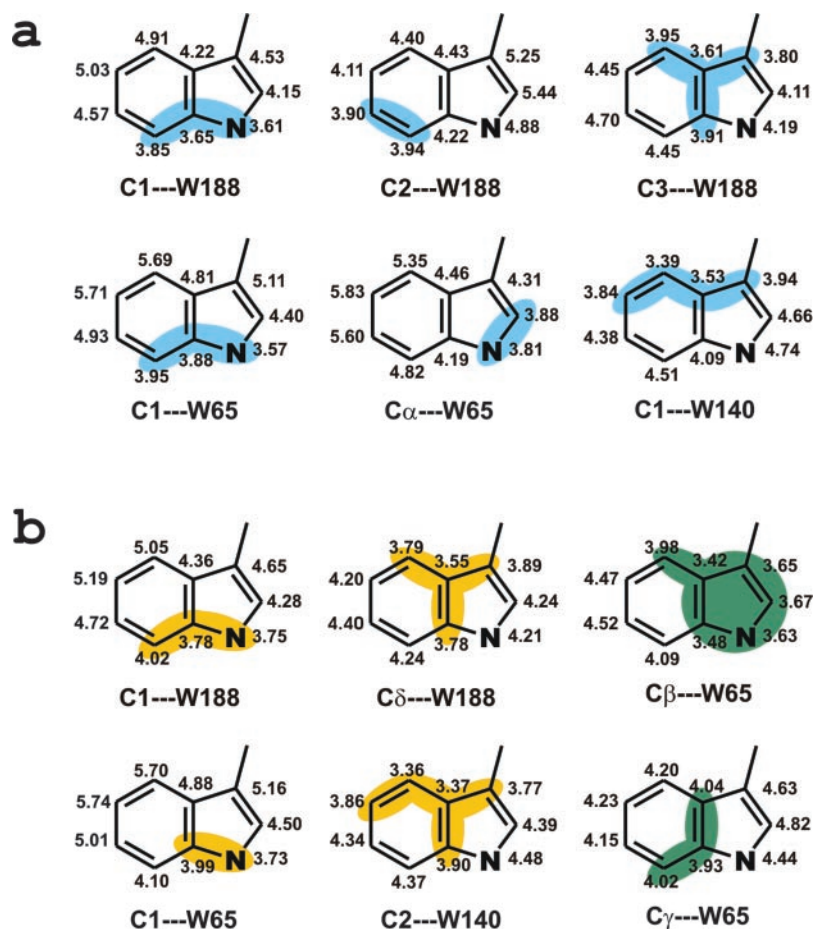


FIG. 5. Carbon-carbon distances in Å between the ligands GB (a) and PB (b) and the carbon atoms of the indole groups of the three tryptophan residues. All atoms of the indole rings involved in cation- π interaction (matching the criterion to be within 3.5–4.0-Å distance) are in blue for GB and yellow for PB (color-coding for the ligand is the same as in Fig. 4). The nomenclature for PB is similar to that for GB except that 3 in GB is, as C δ , part of the proline ring in PB. The quaternary amine of GB forms nine, five, and four contacts, whereas the quaternary amine of PB forms seven, two, and five contacts with the indole groups of Trp¹⁸⁸, Trp⁶⁵, and Trp¹⁴⁰, respectively. PB also forms van der Waals contacts between C β and C γ with the indole ring of Trp⁶⁵ shown in green.

TABLE III
Binding affinities of GB to wild-type ProX and ProX derivatives

	Trp ⁶⁵		Trp ¹⁴⁰		Trp ¹⁸⁸	
	K_D	S.D.	K_D	S.D.	K_D	S.D.
	μM		μM		μM	
Wild type	4	0.1	4	0.1	4	0.1
Trp \rightarrow Phe	4	0.1	3	0.3	4	0.4
Trp \rightarrow Tyr	13	0.6	4	0.5	5	0.2
Trp \rightarrow Ala	50	3.3	56	10	— ^a	—
Trp \rightarrow Leu	—	—	14	1.4	—	—
Trp \rightarrow Asp	—	—	8	0.8	—	—
Trp \rightarrow Glu	—	—	21	2.5	—	—
Trp ⁶⁵ \rightarrow Ala, Trp ¹⁴⁰ \rightarrow Ala	—	—	—	—	—	—

^a —, indicates non-binding ProX mutants. These proteins show no GB binding at the maximum concentration of 110 μM used in the experiments.

phylum), three Rhizobiales (same phylum), and one Cyanobacteria (same kingdom). It can be seen that the tryptophan residues are well conserved in this group of binding proteins, and in some cases they are replaced by tyrosine residues (see Fig. 6). A restraint on the sequence is the proper orientation of the three tryptophan side chains achieved by the surrounding residues, which can also be inferred from the alignment. In ProX the second residue after each of the tryptophans 65 and 188 is a conserved proline in cis-conformation, which allows for a sharply bent backbone. Pro⁶⁷ is placed between the two residues Trp⁶⁵ and His⁶⁹, which both interact with the ligand (see Fig. 6). In the loop containing Trp¹⁴⁰, two conserved glycine and cysteine residues are stabilized by a disulfide link between the two cysteines Cys¹³⁶ and Cys¹⁴². Again the sharp bend of the loop may require Pro¹³⁸, which is also conserved. This entire

motif ¹³⁶CXPWGWC¹⁴² is strictly conserved among the five closest homologues of ProX (see Fig. 6).

Other Cases of Ligands Bound by Cation- π Interaction—Several kinds of ligands with quaternary amines have been observed to form van der Waals contacts with proteins. In a phosphocholine-binding antibody McPC603 (Protein Data Bank accession code 2MCP) two methyl groups of the quaternary amine form contacts with the indole group of Trp¹⁰⁷, and one methyl forms contacts with the phenyl ring of Tyr⁹³.

In the acetylcholine esterase complex with the decamethonium bromide inhibitor (69) and with another inhibitor BW284C51 (70), two quaternary ammonium groups at the ends of the ligands form van der Waals contacts with indole groups. Two methyl groups contact the indole of Trp⁸⁴, and one methyl group contacts the indole of Trp²⁷⁹ at the bottom and the top of the “gorge” (71), respectively. The former of these contacts is believed to resemble that of the quaternary ammonium group of acetylcholine upon catalysis.

To understand whether there is a general architecture of these quaternary amine binding sites in proteins we superimposed ProX-GB with two other structures having completely different folds and substrates. For the comparison we used the structures of the phosphatidylcholine-binding protein (72) and the HP1 chromodomain (73) with Protein Data Bank accession codes 1LN1 and 1KNE, respectively. Because of their different folds only the quaternary amine head group of their ligands was superimposed using LSQMAN (74). Fig. 7 shows those amino acid side chains, which contain at least one atom closer than 4.0 Å to the bound quaternary amine. As can be seen aromatic residues equivalent to Trp⁶⁵ and Trp¹⁸⁸ are also present in the two other proteins, whereas the third residue of the aromatic box is less conserved.

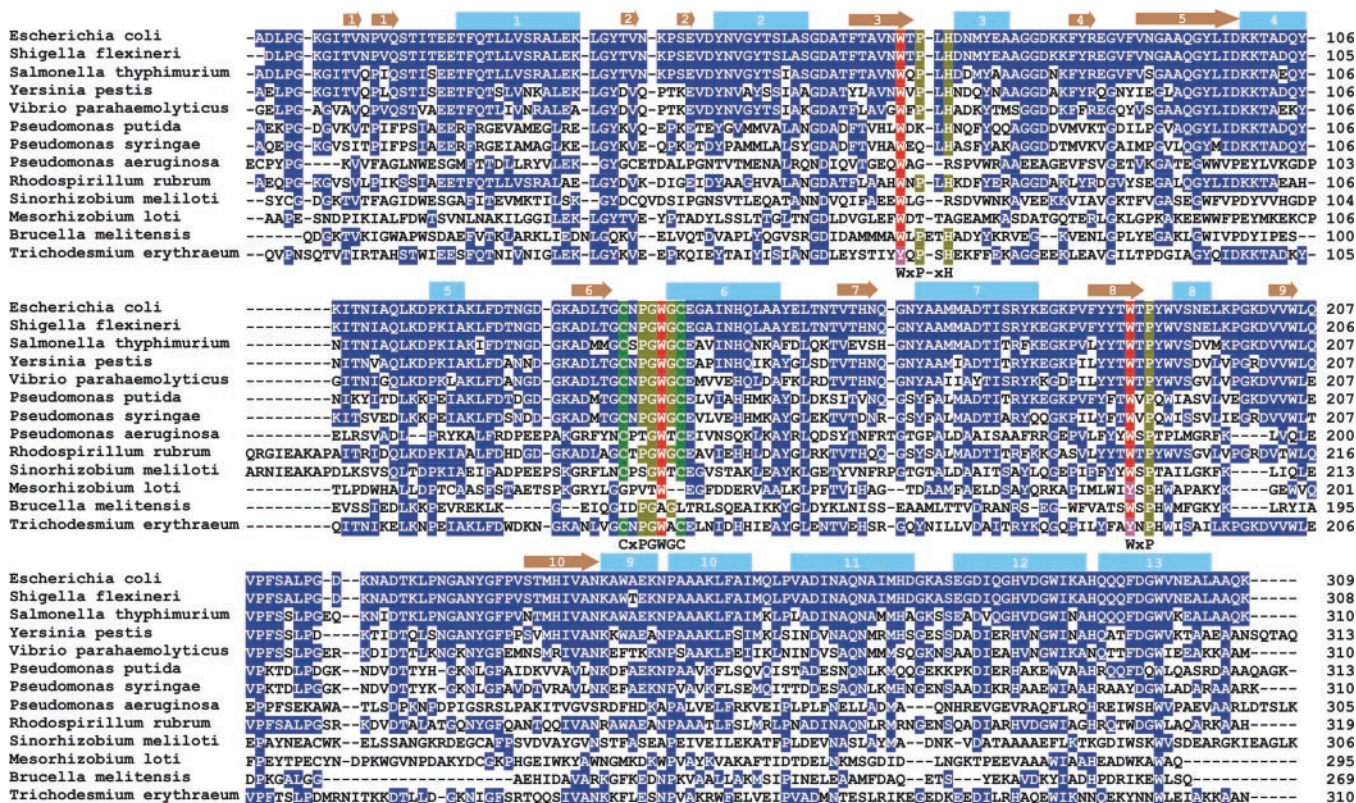


FIG. 6. Alignment of ProX with selected sequences from a homology search. Conserved residues are shown in blue, residues involved in binding of the quaternary amine head group are red (equivalent residues are pink), conserved cysteine residues are green, and structurally important residues are marked olive. Secondary structure elements for the ProX structure were determined using DSSP (82). Helices (light blue) and sheets (brown) are numbered according to Fig. 1. Shown are *E. coli* K12 (NCBI accession no. 16130593), *Shigella flexneri* 2a str. 301 (NCBI accession no. 24113983, 99% identity), *Salmonella typhimurium* LT2 (NCBI accession no. 16766122, 83% identity), *Yersinia pestis* (NCBI accession no. 22125121, 71% identity), *Vibrio parahaemolyticus* (NCBI accession no. 28898502, 66% identity), *Pseudomonas putida* (NCBI accession no. 7542433 51% identity) *Pseudomonas syringae* pv. *tomato* (NCBI accession no. 28870233, 48% identity), *Pseudomonas aeruginosa* PA01 (NCBI accession no. 15600296 24% identity), *Rhodospirillum rubrum* (NCBI accession no. 22968752, 63% identity), *Sinorhizobium meliloti* (NCBI accession no. 8650111, 26% identity), *Mesorhizobium loti* (NCBI 13476104, 25% identity), *Brucella melitensis* (NCBI accession no. 17988895, 25% identity), and *Trichodesmium erythraeum* (NCBI accession no. 23041742, 42% identity).

FIG. 7. Superposition of three quaternary amine binding proteins. The quaternary amine in the center of the binding site (black) was superimposed using LSQMAN (74). Each of the protein residue side chains and the quaternary amine elongations (or parts of them, in brackets) are color-coded: red, ProX (GB); yellow, phosphatidylcholine transfer protein (phosphocholine); blue, chromodomain HP1 (the lysine side chain has three methyl groups attached to the terminal amino group). All amino acid side chains of the proteins that have at least one atom closer than 4 Å to the quaternary amine (QA) are shown in the figure.

DISCUSSION

Binding a Compatible Solute to a Protein—Compatible solutes are of practical interest as they can stabilize labile proteins in a functionally active form *in vitro* over extended periods or act as cryoprotectants. The protective value has been traced to their exclusion from direct contact with the protein surface. As the surface increases in the initial conformational transitions associated with denaturation, denaturation is energetically disfavored in presence of a compatible solute (23, 75–77).

This work addresses the questions as to how such a substance known to avoid interaction with protein surfaces can nevertheless be complexed with high affinity by a protein and what are the critical structural features of such a binding site.

Compared with other small ions or dipolar molecules the quaternary amine group is exceptionally bulky. The positive charge is virtually distributed over a larger volume compared with a metal ion, resulting in a smaller surface potential. The underlying reason for the unfavorable interaction must be a successful competition of water with quaternary ammonium compounds for binding sites on the protein surface. For common protein surfaces the preferred interaction partner may be water because of its small size and consequently stronger surface potential so that it can form an electrically and sterically complementary interface with the protein surface that is better than the quaternary ammonium ion. This is in accord with explanations given for other substances classified as compatible solutes, which are found to be preferentially excluded from

the protein surface. In case of ribonuclease and the compatible solute glycerol, the preferential hydration has been directly proven by neutron small angle scattering (26). Furthermore this exclusion of compatible solutes also resembles the phenomenon of excluded volume, which generally exists in concentrated solutions of large molecules (78).

However, if proteins need to bind such quaternary ammonium cations, a site can be tailored as it is found in ProX. This special site should be a cavity just large enough to accommodate the bulky cation and has to possess an evenly negative surface potential. Indole and phenyl groups from tryptophans, tyrosines, and phenylalanines have been shown to possess such an evenly negative surface potential (79). In ProX, the rectangular indole box is well designed to accommodate quaternary amine ligands and thus provides electrostatic and van der Waals complementarity. An important structural feature are two conserved cis-prolines, which follow the residues Trp⁶⁵ and Trp¹⁸⁸ and might be also in cis-conformation in the related structures (see Fig. 6). These seem to play a crucial role in positioning Trp⁶⁵ and Trp¹⁸⁸ by allowing a sharp bend in the polypeptide backbone to form this almost rectangular box of tryptophan residues as found in ProX. The interaction energy has thus been well optimized under evolutionary pressure.

Mutational Studies—Our mutational data show that at position 188 the phenyl ring of tyrosine or phenylalanine is able to substitute for the indole group, whereas binding is abolished in the non-aromatic mutants. In ProX-GB residue Trp¹⁸⁸ forms more van der Waals contacts (nine) than the other two tryptophans of the box (five and four), and it contacts all methyl groups of the trimethyl betaine ligand (Fig. 5). Trp¹⁸⁸ is the only residue of the box that cannot be replaced by a non-aromatic apolar or acidic residue without a complete loss of binding (Table III). This indicates an essential contribution of the cation- π interaction between Trp¹⁸⁸ and the betaine ligand. As mutational and structural data both hint at a critical influence of this residue, it seems to have a special function in ligand binding.

At the first look positions 65 and 140 appear to be of approximately equal importance for binding of GB, whereas for PB binding position 65 appears to be more important (Fig. 5). In ProX-GB the indole rings of residues Trp⁶⁵ and Trp¹⁴⁰ form similar numbers of van der Waals contacts with the ligand (Fig. 5). Both positions tolerate to a certain degree substitution against alanine and cannot be distinguished by that. However, replacement of the indole group by a bulky aliphatic or a carboxylic group impairs the binding much more strongly in position 65 than in 140 (Table III). This finding can be interpreted in two ways, either as stronger steric or electrostatic restrictions in position 65 or as a more important role of Trp⁶⁵ in ligand binding. The binding site in the closed, ligand-bound conformation appears to offer more space for a large non-aromatic side chain in position 140. An aspartate residue seems to be able to substitute for the tryptophan in position 140 providing electrostatic interactions with a K_D of 8 μ M (Table III). But the larger glutamate residue is less suitable than the aliphatic side chain of leucine, which is most likely for steric reasons. The complete loss of binding activity in the double mutant W65A,W140A demonstrates that at least two aromatic residues are necessary for GB binding. The comparison between ProX and two other quaternary amine-binding proteins being structurally not related shows a convergent evolution of the binding site (Fig. 7). Two aromatic rings almost perpendicular to each other seem to be required, whereas further aromatic residues and their orientation with respect to the ligand determine the strength of the interaction between ligand and protein. In the superposition in Fig. 7 the ProX residues Trp⁶⁵

and Trp¹⁸⁸ are in the positions of the two conserved aromatic residues found also in the two other proteins. This is in accord with the findings of our mutational data, which show that Trp⁶⁵ has a more important role in ligand binding than Trp¹⁴⁰. In summary, it could be shown that Trp¹⁸⁸ in pair with either Trp⁶⁵ or Trp¹⁴⁰ is absolutely necessary for a proper ligand binding, whereas the third tryptophan residue enforces the binding affinity in ProX. The difference in the binding studies between Trp⁶⁵ and Trp¹⁴⁰ reflects their importance in ligand binding.

Quaternary Amine Derivatives as Neurotransmitters—Because of the identical quaternary amine head groups of GB and acetylcholine one tends to compare the interactions between them and their receptors. According to the finding of Dougherty and colleagues (80), the cation- π energy of the acetylcholine quaternary amine bound to Trp¹⁴⁹ in the α -subunit of the nicotinic acetylcholine receptor from *Torpedo californica* is critical for channel response. The structure of the acetylcholine-binding protein from snail (81) that can be taken as a model for the extracellular part of the nicotinic acetylcholine receptor suggests an analogous role for Trp¹⁴³ in acetylcholine-binding protein. However, it is not known yet how the neurotransmitter acetylcholine is exactly bound in the expected aromatic environment. From our data we suggest that Trp¹⁸⁸ in ProX has a function similar to that of Trp¹⁴⁹ in nicotinic acetylcholine receptor and Trp¹⁴³ in acetylcholine-binding protein. Additionally a second aromatic residue in a position similar to that of Trp⁶⁵ in ProX has to be present in the nicotinic acetylcholine receptor to bind the acetylcholine head group properly.

Furthermore from the identity of the head groups we assume a similar exclusion of this part of the acetylcholine molecule from protein surfaces as found for the compatible solute glycine betaine. Only a protein with a highly specific binding site based on cation- π interaction in the form of an aromatic box is able to bind acetylcholine. We thus speculate that quaternary amine derivatives are especially suited to act as neurotransmitters in an environment crowded with a huge number of different proteins like it is in the synaptic cleft where unspecific binding would lead to an inefficient use of the signaling molecule.

REFERENCES

- Kempf, B., and Bremer, E. (1998) *Arch. Microbiol.* **170**, 319–330
- Booth, I. R., and Louis, P. (1999) *Curr. Opin. Microbiol.* **2**, 166–169
- Brown, A. D. (1976) *Bacteriol. Rev.* **40**, 803–846
- Csonka, L. N., and Hanson, A. D. (1991) *Annu. Rev. Microbiol.* **45**, 569–606
- Galinski, E. A., and Trüper, H. G. (1994) *FEMS Microbiol. Rev.* **15**, 95–108
- Bremer, E., and Krämer, R. (2000) in *Bacterial Stress Responses* (Storz, G., and Hengge-Aronis, R., eds) pp. 79–97, American Society for Microbiology Press, Washington, D. C.
- Welsh, D. T. (2000) *FEMS Microbiol. Rev.* **24**, 263–290
- Wood, J. M. (1999) *Microbiol. Mol. Biol. Rev.* **63**, 230–262
- Record, M. T., Jr., Courtenay, E. S., Cayley, D. S., and Guttman, H. J. (1998) *Trends Biochem. Sci.* **23**, 143–148
- Lippert, K., and Galinski, A. A. (1992) *Appl. Microbiol. Biotechnol.* **37**, 61–65
- Caldas, T., Demont-Caulet, N., Ghazi, A., and Richarme, G. (1999) *Microbiology* **145**, 2543–2548
- Canovas, D., Borges, N., Vargas, C., Ventosa, A., Nieto, J. J., and Santos, H. (1999) *Appl. Environ. Microbiol.* **65**, 3774–3779
- Bourot, S., Sire, O., Trautwetter, A., Touze, T., Wu, L. F., Blanco, C., and Bernard, T. (2000) *J. Biol. Chem.* **275**, 1050–1056
- Canovas, D., Fletcher, S. A., Hayashi, M., and Csonka, L. N. (2001) *J. Bacteriol.* **183**, 3365–3371
- Mendum, M. L., and Smith, L. T. (2002) *Appl. Environ. Microbiol.* **68**, 813–819
- Da Costa, M. S., Santos, H., and Galinski, E. A. (1998) *Adv. Biochem. Eng. Biotechnol.* **61**, 117–153
- Roberts, M. F. (2000) *Front. Biosci.* **5**, 796–812
- Burg, M., Kwon, E., and Kiltz, D. (1997) *Annu. Rev. Physiol.* **59**, 437–455
- Rhodes, S., and Hanson, A. D. (1993) *Annu. Rev. Plant Physiol. Plant Mol. Biol.* **44**, 357–384
- Hohmann, S. (2002) *Int. Rev. Cytol.* **215**, 149–187
- Le Rudulier, D., Strøm, A. R., Dandekar, A. M., Smith, L. T., and Valentine, R. C. (1984) *Science* **224**, 1064–1068
- Yancey, P. H. (1994) in *Cellular and Molecular Physiology of Cell Volume Regulation* (Strange, K., ed) pp. 81–109, CRC Press, Inc., Boca Raton, FL
- Arakawa, T., and Timasheff, S. N. (1985) *Biochem. J.* **47**, 411–414
- Qu, Y., Bolen, C. L., and Bolen, D. W. (1998) *Proc. Natl. Acad. Sci. U. S. A.* **95**, 9268–9273

25. Bolen, D. W., and Baskakov, I. V. (2001) *J. Mol. Biol.* **310**, 955–963
26. Lehmann, M. S., and Zaccai, G. (1984) *Biochemistry* **23**, 1939–1942
27. Csonka, L. N., and Epstein, W. (1996) in *Escherichia coli and Salmonella. Cellular and Molecular Biology* (Neidhard, F. C., Curtiss, R., III, Ingraham, J. L., Lin, E. C. C., Low, K. B., Magasanik, B., Reznikoff, W. S., Riley, M., Schaechter, M., and Umberger, H. E., eds) Vol. 1, pp. 1210–1223, American Society for Microbiology Press, Washington, D. C.
28. Sleator, R. D., and Hill, C. (2002) *FEMS Microbiol. Rev.* **26**, 49–71
29. Perroud, B., and Le Rudulier, D. (1985) *J. Bacteriol.* **161**, 393–401
30. Lucht, J. M., and Bremer, E. (1994) *FEMS Microbiol. Lett.* **14**, 3–20
31. Culham, D. E., Lasby, B., Marangoni, A. G., Milner, J. L., Steer, B. A., van Nues, R. W., and Wood, J. M. (1993) *J. Mol. Biol.* **229**, 268–276
32. May, G., Faatz, E., Villarejo, M., and Bremer, E. (1986) *Mol. Gen. Genet.* **205**, 225–233
33. Gowrishankar, J. (1989) *J. Bacteriol.* **171**, 1923–1931
34. Higgins, C. F. (1992) *Annu. Rev. Cell Biol.* **8**, 67–113
35. Boos, W., and Lucht J. M. (1996) in *Escherichia coli and Salmonella. Cellular and Molecular Biology* (Neidhard, F. C., Curtiss, R., III, Ingraham, J. L., Lin, E. C. C., Low, K. B., Magasanik, B., Reznikoff, W. S., Riley, M., Schaechter, M., and Umberger, H. E., eds) pp. 1175–1209, American Society for Microbiology Press, Washington, D. C.
36. Faatz, E., Middendorf, A., and Bremer, E. (1988) *Mol. Microbiol.* **2**, 265–279
37. Barron, A., Jung, J. U., and Villarejo M. (1987) *J. Biol. Chem.* **262**, 11841–11846
38. Haardt, M., Kempf, B., Faatz, E., and Bremer, E. (1995) *Mol. Gen. Genet.* **246**, 783–786
39. Fetsch, E. E., and Davidson, A. L. (2002) *Proc. Natl. Acad. Sci. U. S. A.* **99**, 9685–9690
40. Jebbar, M., Talibart, R., Gloux, K., Bernard, T., and Blanco, C. (1992) *J. Bacteriol.* **174**, 5027–5035
41. Magnusson, U., Chaudhuri, B. N., Ko, J., Park, C., Jones, A., and Mowbray, S. L. (2002) *J. Biol. Chem.* **277**, 14077–14084
42. Björkman, A. J., and Mowbray, S. L. (1998) *J. Mol. Biol.* **279**, 651–664
43. Higgins, C. F., Sutherland, L., Cairney, J., and Booth, I. R. (1987) *J. Gen. Microbiol.* **133**, 305–310
44. Breed, J., Kneip, S., Gade, J., Welte, W., and Bremer, E. (2001) *Acta Crystallogr. Sect. D Biol. Crystallogr.* **57**, 448–450
45. Dulaney, E. L., Dulaney, D. D., and Rickes, E. L. (1968) *Dev. Ind. Microbiol.* **9**, 260–269
46. Neu, H. C., and Heppel, L. A. (1965) *J. Biol. Chem.* **240**, 3685–3692
47. Silhavy, T. J., Berman, M. L., and Enquist, L. W. (1984) *Experiments with Gene Fusions*, pp. 18–27, Cold Spring Harbor Laboratories, Cold Spring Harbor, NY
48. Diederichs, K., and Karplus, P. A. (1997) *Nat. Struct. Biol.* **4**, 269–275
49. Bremer, E., Silhavy, T. J., and Weinstock, G. M. (1988) *Gene (Amst.)* **71**, 177–186
50. Weiss, M. S., and Hilgenfeld, R. (1997) *J. Appl. Crystallogr.* **30**, 203–205
51. Sanger, F., Nicklen, S., and Coulson, A. R. (1977) *Proc. Natl. Acad. Sci. U. S. A.* **74**, 5463–5467
52. Richarme, G., and Kepes, A. (1983) *Biochim. Biophys. Acta* **742**, 16–24
53. Kabsch, W. (1993) *J. Appl. Crystallogr.* **26**, 795–800
54. Terwilliger, T. C., and Berendzen, J. (1999) *Acta Crystallogr. Sect. D Biol. Crystallogr.* **55**, 849–861
55. Cowtan, K. (1994) *Joint CCP4 and ESF-EACBM Newslett. Protein Crystallogr.* **31**, 34–38
56. Jones, T. A., Zou, J. Y., Cowan, S. W., and Kjeldgaard, M. (1991) *Acta Crystallogr. Sect. A* **47**, 110–119
57. Murshudov, G. N., Vagin, A. A., and Dodson, E. J. (1997) *Acta Crystallogr. Sect. D Biol. Crystallogr.* **53**, 240–255
58. Laskowski, R. A., MacArthur, M. W., Moss, D. S., and Thornton, J. M. (1993) *J. Appl. Crystallogr.* **26**, 283–291
59. Kraulis, P. J. (1991) *J. Appl. Crystallogr.* **24**, 946–950
60. Esnouf, R. M. (1997) *J. Mol. Graph. Model.* **15**, 132–134
61. Merritt, E. A., and Bacon, D. J. (1997) *Methods Enzymol.* **277**, 505–524
62. Altschul, S. F., Gish, W., Miller, W., Myers, E. W., and Lipman, D. J. (1990) *J. Mol. Biol.* **215**, 403–410
63. Quiocho, F. A., and Ledvina, P. S. (1996) *Mol. Microbiol.* **20**, 17–25
64. Clarke, T. E., Ku, S.-Y., Dougan, D. R., Vogel, H. J., and Tari, L. W. (2000) *Nat. Struct. Biol.* **7**, 287–291
65. Borths, E. L., Locher, K. P., Lee, A. T., and Rees, D. C. (2002) *Proc. Natl. Acad. Sci. U. S. A.* **99**, 16642–16647
66. Berman, H. M., Westbrook, J., Feng, Z., Gilliland, G., Bhat, T. N., Weissig, H., Shindyalov, I. N., and Bourne, P. E. (2000) *Nucleic Acids Res.* **28**, 235–242
67. Li, A.-J., and Nussinov, R. (1998) *Proteins* **32**, 111–127
68. Momma, K., Mikami, B., Mishima, Y., Hashimoto, W., and Murata, K. (2002) *J. Mol. Biol.* **316**, 1051–1059
69. Harel, M., Schalk, I., Ehret-Sabatier, L., Bouet, F., Goeldner, M., Hirth, C., Axelsen, P. H., Silman, I., and Sussman, J. L. (1993) *Proc. Natl. Acad. Sci. U. S. A.* **90**, 9031–9035
70. Felder, C. E., Harel, M., Silman, I., and Sussman, J. L. (2002) *Acta Crystallogr. Sect. D Biol. Crystallogr.* **58**, 1765–1771
71. Ripoli, D. R., Faerman, C. H., Axelsen, P. H., Silman, I., and Sussman, J. L. (1993) *Proc. Natl. Acad. Sci. U. S. A.* **90**, 5128–5132
72. Roderick, S. L., Chan, W. W., Agate, D. S., Olsen, L. R., Vetting, M. W., Rajashankar, K. R., and Cohen, D. E. (2002) *Nat. Struct. Biol.* **9**, 507–511
73. Jacobs, S. A., and Khorasanizadeh, S. (2002) *Science* **295**, 2080–2083
74. Kleywegt, G. J., and Jones, T. A. (1994) *Joint CCP4 and ESF-EACBM Newslett. Protein Crystallogr.* **31**, 9–14
75. Lee, J. C., and Timasheff, S. N. (1981) *J. Biol. Chem.* **256**, 7193–7201
76. Timasheff, S. N. (1993) *Annu. Rev. Biophys. Biol. Struct.* **22**, 67–97
77. Kendrick, B. S., Chang, B. S., Arakawa, T., Peterson, B., Randolph, T. W., Manning, M. C., and Carpenter, J. F. (1997) *Proc. Natl. Acad. Sci. U. S. A.* **94**, 11917–11922
78. Minton, A. P. (2001) *J. Biol. Chem.* **276**, 10577–10580
79. Mecozzi, S., West, A. P., Jr., and Dougherty, D. (1996) *Proc. Natl. Acad. Sci. U. S. A.* **93**, 10566–10571
80. Zhong, W., Gallivan, J. P., Zhang, Y., Li, L., Lester, H. A., and Dougherty, D. A. (1998) *Proc. Natl. Acad. Sci. U. S. A.* **95**, 12088–150202
81. Brejc, K., van Dijk, W. J., Klaassen, R. V., Schuurmans, M., van der Oost, J., Smit, A. B., and Sixma, T. K. (2001) *Nature* **411**, 269–276
82. Kabsch, W., and Sander, C. (1983) *Biopolymers* **22**, 2577–2637